ACS MEASUREMENT SCIENCE Au
AN OPEN ACCESS JOURNAL OF THE AMERICAN CHEMICAL SOCIETY

Open Access
This article is licensed under CC-BY-NC-ND 4.0

pubs.acs.org/measureau
Article

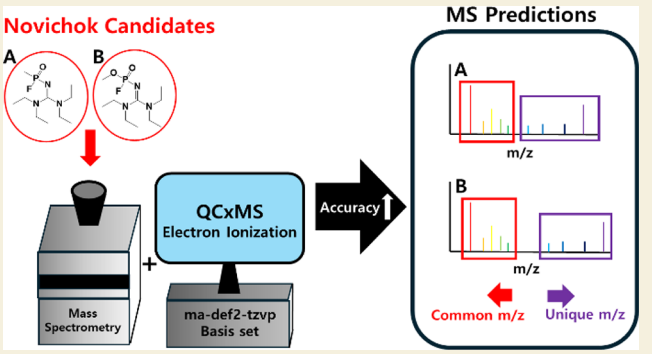
Quantum Chemical Mass Spectral Predictions of Novichok Agents after Experimental Validation and Analysis

Sungsoo Kim, Moon Sik Shin, Seonghoon Hong, Janghyuk Moon, Seungbum Jo,* and Keunhong Jeong*

Cite This: ACS Meas. Sci. Au 2025, 5, 378−387
Read Online

ACCESS | Metrics & More | Article Recommendations | Supporting Information

ABSTRACT: The identification of chemical warfare agents, particularly Novichok variants, presents significant challenges due to the inherent dangers and practical limitations of experimental analysis. This study advances a computational approach using quantum chemistry electron ionization mass spectrometry (QCxMS, x = EI) to predict the electron ionization mass spectra (EIMS) of these compounds. We obtained experimental mass spectral data from three synthesized Novichok compounds, providing a crucial benchmark for validating computational predictions. Through systematic comparison of the experimental and predicted spectra, we evaluated how the incorporation of additional polarization functions and expanded valence space in basis sets influences prediction accuracy. Our investigation demonstrated that more complete basis sets yielded significantly improved matching scores across seven compounds while maintaining consistent functional parameters for ionization potential (IP) calculations. Comprehensive analysis of mass spectral patterns revealed distinct correlations between the molecular structure and fragmentation behavior. We identified characteristic patterns in both high and low *m*/*z* regions that correspond to specific structural features, enabling the development of a systematic framework for spectral interpretation. This understanding of the fragmentation mechanisms allowed for the prediction of mass spectra for four additional compounds with varying structural complexity. The strong correlation between the predicted and experimental results for the synthesized compounds validates this computational approach as a promising tool for the rapid identification of new chemical agents without requiring extensive experimental analysis. This methodology represents a significant advancement in our ability to identify and characterize emerging chemical threats while minimizing exposure risks to research personnel.



KEYWORDS: *novichok agents, electron ionization mass spectrometry (EIMS), quantum chemistry electron ionization mass spectrometry (QCxMS), basis set optimization(ma-def2-tzvp), fragmentation pattern analysis*

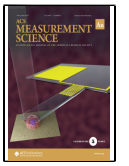
Downloaded via CHUNG-ANG UNIV on June 27, 2025 at 07:23:48 (UTC).
See https://pubs.acs.org/sharingguidelines for options on how to legitimately share published articles.

1. INTRODUCTION

The growing complexity and sophistication in the development of chemical warfare agents, particularly the new types of nerve agent series, has escalated the global chemical threat landscape significantly.[1−4] These agents are characterized by their structural versatility, enabling modifications that result in hundreds or even tens of thousands of potential variants.[3,4] Such variability presents a formidable challenge in chemical defense, as effective preparedness is critically dependent on the ability to rapidly and accurately identify these hazardous substances.[5−8] Conventionally, identification processes have relied heavily on mass spectrometry (MS), a technique that requires the availability of extensive spectral libraries for accurate matching of chemical signatures.[9,10] However, the development of comprehensive spectral libraries for these compounds faces severe practical limitations due to the extreme toxicity of the agents, the high risk of synthesis and analysis, and strict regulatory requirements limiting the facilities capable of conducting such work.[11,12] These constraints make it impractical and potentially dangerous to synthesize and analyze all of the possible variants for library development.

Moreover, while previous computational studies have made valuable contributions to understanding Novichok agents, they have been limited by the absence of experimental mass spectral data for validation. The selection of an appropriate basis set is particularly critical when dealing with organophosphorus

Received: March 3, 2025
Revised: May 12, 2025
Accepted: May 13, 2025
Published: May 23, 2025



ACS Publications
© 2025 The Authors. Published by American Chemical Society

https://doi.org/10.1021/acsmeasuresciau.5c00026
ACS Meas. Sci. Au 2025, 5, 378−387

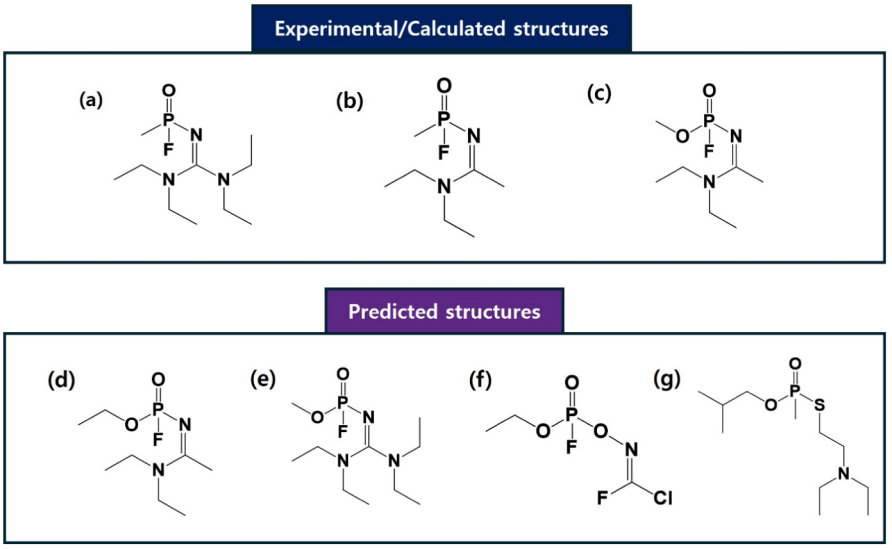


Figure 1. Molecular structure of studied nerve agents (upper structures are representing (a) **compound 1**: *N*-(bis(diethylamino)methylidene)-*P*-methylphosphonamidic fluoride, (b) **compound 2**: *N*-(1-(diethylamino)ethylidene)-*P*-methylphosphonamidic fluoride, (c) **compound 3**: methyl *N*-(1-(diethylamino)ethylidene)phosphoramidofluoridate. Lower structures represent (d) **compound 4**: ethyl *N*-(1-(diethylamino)ethylidene)-phosphoramidofluoridate, (e) **compound 5**: methyl (bis(diethylamino)methylene)phosphoramidofluoridate, (f) **compound 6**: (*Z*)-ethyl ((chlorofluoromethylene)amino)oxyphosphonofluoridate, (g) **compound 7**: *S*-(2-(diethylamino)ethyl) *O*-isobutyl methylphosphonothioate).

compounds such as Novichok agents, as these molecules contain elements with complex electronic structures and exhibit intricate fragmentation patterns. Previous computational studies on chemical warfare agents have often prioritized computational efficiency over accuracy by using minimal basis sets, potentially compromising the reliability of their predictions.

In response to these challenges, this study presents the first experimental validation of QCxMS predictions using actual synthesized Novichok compounds. Through systematic analysis of mass spectral fragmentation patterns based on functional groups and molecular weight distributions, we established a comprehensive framework for predicting the mass spectra of novel structures. This approach enables the identification of characteristic fragmentation patterns associated with specific structural features, such as methyl, methoxy, and ethoxy groups bound to phosphine at higher m/z values and ethyl groups attached to nitrogen in guanidine and amidine structures at lower m/z values. Such a systematic understanding is crucial for enhancing our predictive capabilities for new chemical agents without requiring their actual synthesis. We focus on synthesizing three recently identified Novichok compounds on a microscale and subsequently acquiring their electron ionization mass spectra (Figure 1). These three compounds (**compounds 1−3**) were selected based on their structural and regulatory significance, as they were recently added to Schedule 1.A.13 and 1.A.14 of the Annex on Chemicals to the Chemical Weapons Convention (CWC).[13−15] These agents exemplify the core phosphoramidofluoridate and phosphonamidofluoridate frameworks characteristic of the A- and B-series Novichok agents and were selected for their synthetic accessibility under microscale conditions. The selection is further supported by recent experimental work by Chernicharo et al.,[16] who provided validated EI-MS spectra for structurally similar compounds.

To broaden our study, we also included four novel agents (**compounds 4−7**) that preserve key functional motifs while diversifying the structural space. These candidates were selected based on predicted fragmentation behavior, chemical relevance, and the absence of prior spectral characterization.[17−19] This combination of validated and novel compounds enabled robust benchmarking of predictive models and exploratory extension of the models into chemically plausible but uncharacterized Novichok analogues.

Employing the QCxMS (x = EI) program,[20] we undertook a series of predictive spectral calculations, with a particular emphasis on diversifying the ionization potential (IP) calculation methods.[20−22] The objective of this research was to evaluate which computational techniques most effectively enhance the accuracy of the spectral predictions. This was assessed by comparing the matching scores between the predicted and experimentally obtained spectra.

The development of highly accurate predictive methodologies is particularly crucial, given the aforementioned dangers and practical limitations of creating comprehensive experimental spectral libraries for these compounds. By enhancing the reliability of computational predictions, this approach offers a safer and more practical alternative to extensive experimental characterization of these hazardous materials. The results from this study are anticipated to refine the methodologies employed for the spectral identification of new nerve agents and other similar compounds. Building on the methods that produced the best-matching scores, we also projected the EIMS for four additional new nerve agent candidates, which we then used to aid in the identification of those specific structures. By developing a more reliable and comprehensive framework for the prediction of chemical spectra, this work aims to strengthen our preparedness for and response to chemical threats. Ultimately, this research provides a robust and innovative tool for the rapid identification of novel chemical agents, enhancing security measures and environmental safety protocols in various settings while minimizing the need for dangerous experimental work.

https://doi.org/10.1021/acsmeasuresciau.5c00026
ACS Meas. Sci. Au 2025, 5, 378−387

2. METHODS

2.1. Experiment

All chemicals and reagents required for the microsynthesis of (a), (b), and (c) were purchased from Sigma-Aldrich (Seoul, Korea). Nerve agents were synthesized in our laboratory, and the purity of the prepared materials was >95%. GC/MS analyses were performed using an Agilent 7890A gas chromatograph equipped with a 5975C quadrupole mass selective detector (MSD; Agilent Technologies, Inc., Santa Clara, CA, USA), an HP-5MS (5% phenyl, 95% dimethylpolysiloxane, Agilent's J and W Scientific) capillary column (30 m, 0.25 mm i.d. and 0.25 μm film thickness), and helium as the carrier gas at a constant flow rate of 1.8 mL min^{-1}. The oven temperature was set at 40 °C for 1 min, then ramped to 300 °C at 10 °C/min, and held for 1 min. The samples were injected in splitless mode at an injection temperature of 250 °C. The temperatures of the EI source and analyzer were kept at 230 and 150 °C, respectively. The scan range was m/z 35−500.

2.2. QCxMS (x = EI) Calculation

To simulate the electron ionization (EI) mass spectra of novel nerve agents (Figure 1), we adopted a quantum chemical molecular dynamics-based protocol using the QCxMS package (v5.2.1),[21,23] based on the QCEIMS methodology developed by Grimme and coworkers. As a preliminary step, initial ground-state geometries were optimized using density functional theory (DFT)[24] at the B3LYP/6-311+G(3df,2pd) level[25] of theory. These calculations provided key input parameters for the QCxMS simulation, including optimized molecular geometries and ionization potential (IP). The IP values were computed separately using the ORCA package, as they are essential for determining charge distribution in fragment ions.[26] All geometry optimizations were conducted in the gas phase without symmetry constraints.

Following geometry optimization, the electron ionization process was simulated using the QCxMS workflow, which integrates Born−Oppenheimer molecular dynamics, stochastic sampling, and statistical thermodynamics. The simulation consists of four major steps: (1) canonical ensemble (NVT) equilibration of the neutral molecule at 500 K, (2) generation of initial geometries and velocities for ionization, (3) assignment of internal excess energy (IEE) using a Poisson distribution[21] with a default maximum of 70 eV, and (4) production of fragmentation trajectories under a microcanonical ensemble (NVE) to simulate mass spectral fragments. The resulting fragment IPs[20,21] were computed to derive statistical charges via a Boltzmann distribution model, which were then used to construct the simulated mass spectrum. The QCxMS ultimately generates predicted mass-to-charge(m/z) values and their corresponding relative intensities, which compose the simulated electron ionization mass spectra, and calculates a matching score by comparing the simulated spectrum with the experimental data.

To compute forces along the dynamics, we applied the semi-empirical GFN2-xTB method,[27] which has shown reliability for large-scale fragmentation studies while significantly reducing computational cost. For comparison and assessment of basis set effects on predicted spectra, additional DFT calculations were performed using the PBE0-D3 functional[28,29] with Karlsruhe basis sets[30] (def2-SVP, def2-TZVP, and ma-def2-TZVP) in IP calculations via the ORCA package (v5.0.4).[31] Variation in the basis set directly influenced the computed IP, which in turn affected charge distribution and the resulting peak intensities in the simulated spectra.[20,22,26,32] The statistical charge model ensures that each simulated fragmentation trajectory contributes a normalized +1 charge, distributed among possible ionized fragments. All simulations employed a standard electron energy of 70 eV and an initial temperature of 500 K for the equilibration. The ionization excess energy (IEE) per atom was set at 0.6 eV, as per the QCxMS default parameters.

3. RESULTS AND DISCUSSION

Figure 2 presents the experimental electron ionization (EI) mass spectra of three structurally distinct Novichok candidates,

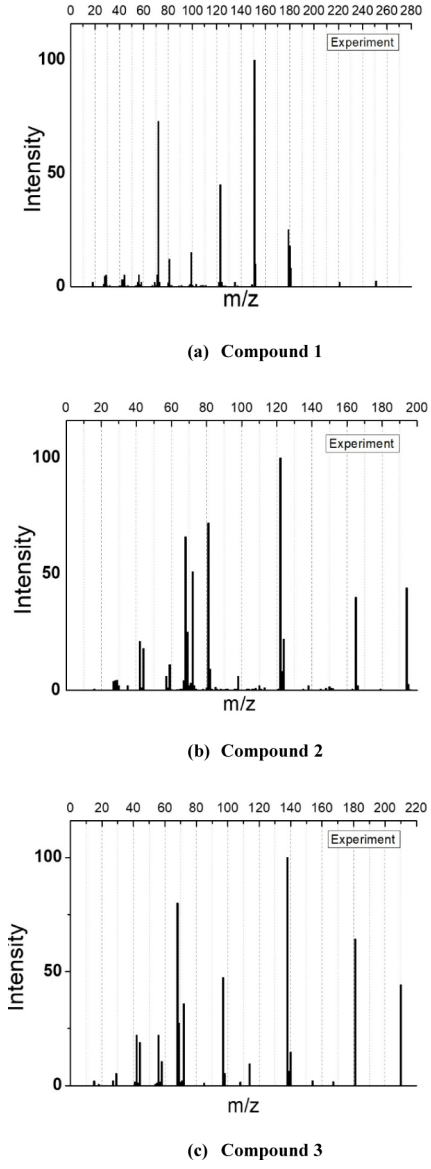


Figure 2. Experimental spectrum (electron ionization).

compounds 1, **2,** and **3**. These compounds share a common structural motif featuring a fluorine atom as a leaving group bound to phosphorus, yet they exhibit distinct mass spectral signatures arising from their unique molecular architectures. The molecular framework can be categorized into two main structural classes: guanidine-based (**compound 1**) and amidine-based (**compounds 2, 3**) structures. The guanidine-based structure in **compound 1** contains two $N(CH_2CH_3)_2$ groups bound to the central carbon, while the amidine-based structures in **compounds 2, 3** feature a single $N(CH_2CH_3)_2$ group with an additional methyl substituent. Systematic analysis of these base structures guided our prediction strategy for **compound 4** and **5**. For the guanidine framework, we extended our analysis from **compound 1** to predict **compound 5**, where the key structural modification involves replacing the P-CH_3 group with P-OCH_3. Similarly, within the amidine

https://doi.org/10.1021/acsmeasuresciau.5c00026
ACS Meas. Sci. Au 2025, 5, 378−387

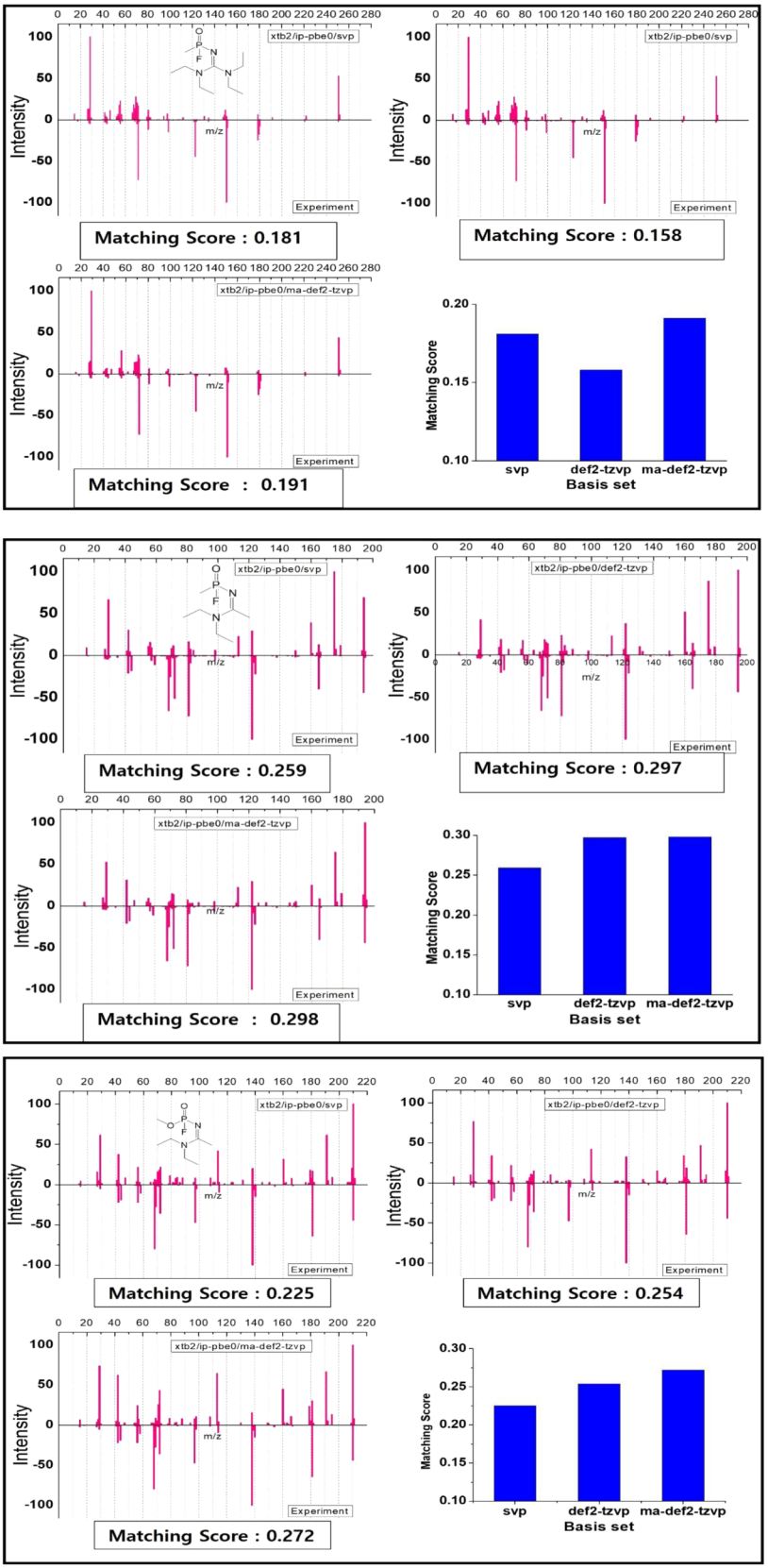


Figure 3. Electron ionization spectrum and matching score values between experimental and calculated electron ionization spectrum of **compound 1**, **compound 2**, and **compound 3**.

framework, we analyzed the spectral impact of progressive modifications from P-CH_3 (**compound 2**) to P-OCH_3 (**compound 3**), which informed our prediction of compound (d) containing P-OCH_2CH_3. This systematic variation of substituents allowed us to establish clear structure-spectrum relationships.

https://doi.org/10.1021/acsmeasuresciau.5c00026
ACS Meas. Sci. Au 2025, 5, 378−387

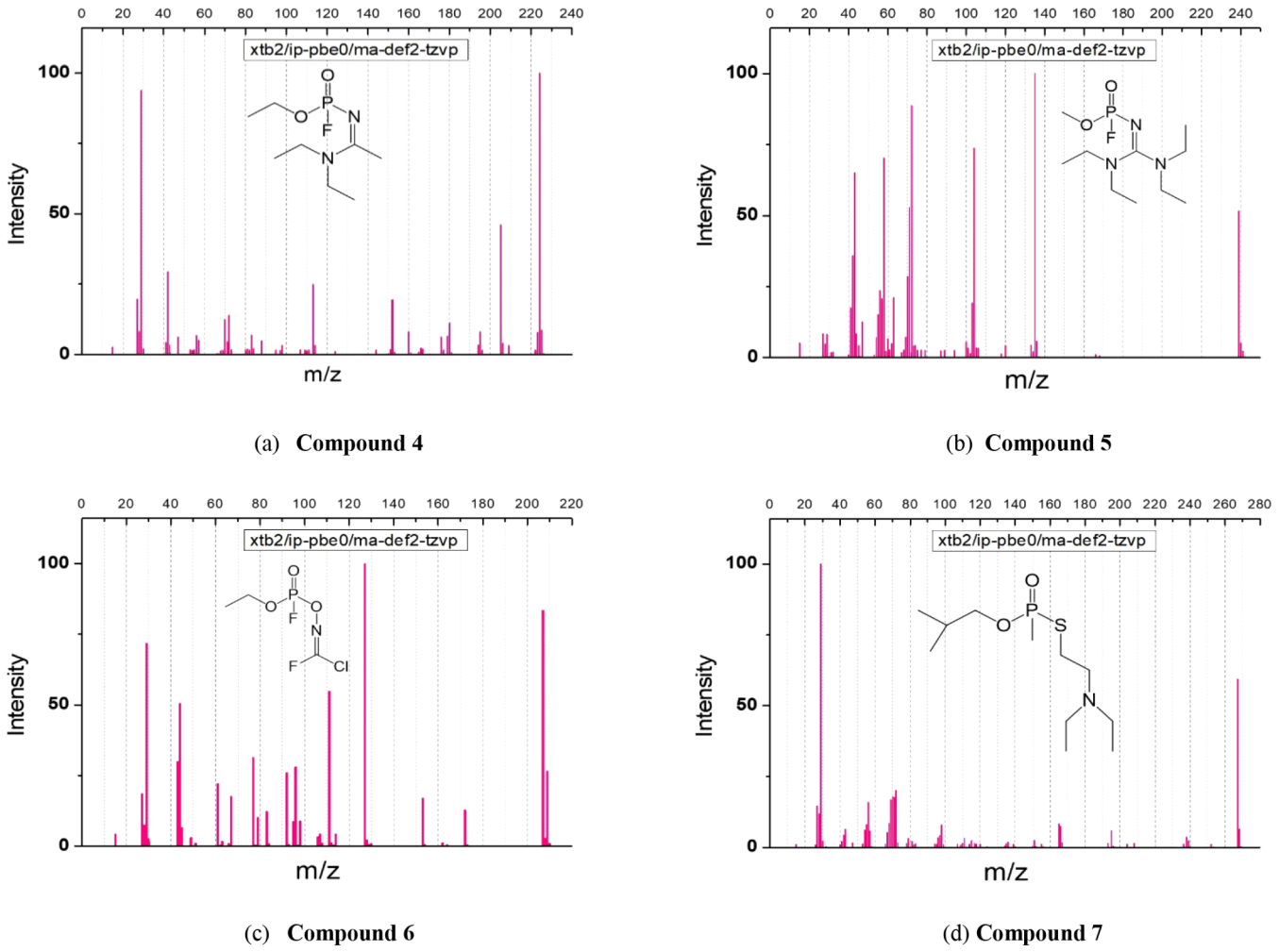


Figure 4. Predicted electron ionization spectrum of **compound 4**−**compound 7**. Employing the validated ma-def2-tzvp basis set methodology, we extended our analysis to predict the mass spectra of **compound 4**−**compound 7**. The high accuracy demonstrated in predicting the experimental spectra of **compound 1**−**compound 3** provides a robust foundation for these predictions. Figure 4 presents the computationally predicted mass spectra, revealing distinct fragmentation patterns that reflect the structural variations among these compounds. For **compound 4**, which shares the guanidine core structure with **compound 1**, the predicted spectrum exhibits characteristic fragmentation patterns arising from the bis(diethylamino)methylidene moiety. The key difference lies in the presence of the P-OCH_3 group instead of P-CH_3, resulting in diagnostic peaks at higher m/z values that reflect this structural modification. The electronic effects of the methoxy substitution influence both the initial ionization process and subsequent fragmentation pathways, leading to distinctive spectral features that differentiate it from **compound 1**.

The mass spectral differences observed between these compounds demonstrate remarkable sensitivity to structural modifications. Particularly, noteworthy is the comparison between **compounds 2** and **3**, where the substitution of P-CH_3 with P-OCH_3 leads to significant alterations in both fragmentation patterns and relative peak intensities. The observed spectral variations can be attributed to the fundamental differences in bond dissociation energies between P−C and P−O bonds alongside the distinct electronic effects of methyl versus methoxy substituents on the phosphorus center. These electronic and structural factors significantly influence the molecular orbital interactions that govern the ionization and fragmentation pathways.

This high structural sensitivity presents both challenges and opportunities for spectral prediction. While it complicates the development of universal prediction models, it also provides distinctive spectral fingerprints that can aid in structural identification. To address these complexities, we employed the QCxMS computational method across multiple basis sets, enabling analysis and prediction of not only compounds (a), (b), and (c), but also structurally related compounds (d) and (e), as well as the more structurally divergent compounds (f) and (g) shown in Figure 1. This comprehensive approach allows for a systematic evaluation of prediction accuracy across a broad range of structural variations within the Novichok family.

Figure 3 presents a comprehensive analysis of how different basis sets influence the accuracy of the QCxMS predictions for Novichok compounds. Our investigation builds upon previous computational studies of Novichok molecules, which were limited to PBE0 functionals with the svp basis set.[22] The inherent limitations of using only the basic svp basis set become apparent when examining the electron density distributions and orbital interactions critical for accurate IP calculations, particularly for molecules containing phosphorus and multiple nitrogen atoms with complex electronic structures.

To address these limitations, we systematically evaluated three basis sets of increasing complexity and computational demand: svp, def2-tzvp, and ma-def2-tzvp. The ma-def2-tzvp

https://doi.org/10.1021/acsmeasuresciau.5c00026
ACS Meas. Sci. Au 2025, 5, 378−387

basis set, with its augmented functions and triple-ζ valence quality, provides a more complete description of the molecular orbitals involved in the ionization processes. This enhanced electronic structure description is particularly crucial for accurately representing the electron density around the phosphorus center and the multiple nitrogen atoms in Novichok compounds, which significantly influence fragmentation patterns. The superiority of the ma-def2-tzvp basis set is quantitatively demonstrated through matching scores between the experimental and calculated spectra. For **compound 1**, featuring a guanidine structure, the ma-def2-tzvp basis set achieved a matching score of 0.191, significantly outperforming the def2-tzvp basis set's score of 0.158. This improvement can be attributed to a better representation of the electron-rich guanidine moiety and its interaction with the phosphorus center. Similar trends were observed for **compound 2** and **compound 3**, where the ma-def2-tzvp basis set consistently yielded the highest-matching scores, while the basic svp basis set produced the lowest scores. This pattern suggests that the enhanced basis set particularly improves the description of electronic interactions in the amidine structural motif common to both compounds. The correlation between basis set completeness and prediction accuracy is not merely statistical but reflects fundamental quantum mechanical principles. The ma-def2-tzvp basis set's superior performance likely stems from its better description of electron correlation effects and improved representation of molecular orbital interactions during the ionization process. These factors are crucial for accurately predicting both the primary ionization events and the subsequent fragmentation pathways that determine the mass spectral patterns.

Based on these findings, we employed the ma-def2-tzvp basis set for predicting the mass spectra of novel **compound 4** through **compound 7**. This choice was driven by the basis set's demonstrated ability to accurately capture the electronic structure features that govern ionization and fragmentation behaviors in these complex organophosphorus compounds. The validation of this approach through experimental comparison for **compound 1**, **compound 2**, and **compound 3** provides confidence in the reliability of predictions for structurally related compounds.

Compound 4 represents a structural extension of amidine-based **compound 2** and **compound 3**, featuring a P-OCH_2CH_3 group. The predicted spectrum shows fragmentation patterns consistent with the established trends observed in the experimental spectra of compounds **compound 2** and **compound 3**. The presence of the ethoxy group introduces additional fragmentation pathways, particularly evident in the higher mass region where P−O bond cleavage processes dominate. The systematic relationship between structural modifications and spectral changes observed in the experimental compounds provides confidence in these predictions. **Compound 6** and **compound 7** represent more diverse structural variations within the Novichok framework. **Compound 6** incorporates a unique chlorofluoromethylene group, while **compound 7** features a methylphosphonothioate structure. The predicted spectra for these compounds reflect their distinct molecular architectures, with characteristic fragmentation patterns arising from their unique structural features. The presence of sulfur in **compound 6** and chlorine in **compound 7** leads to distinctive isotopic patterns in their respective mass spectra, providing additional structural confirmation points. The comprehensive fragmentation analysis presented in Figures S1 and S2 provides detailed insights into the relationship between molecular structure and mass spectral behavior. Figure S1 highlights the primary fragmentation pathways observed in the experimental spectra, while Figure S2 presents the complete set of predicted fragmentations, including secondary and tertiary decomposition products. This detailed analysis establishes a framework for understanding and predicting the mass spectral behavior of novel Novichok variants, potentially eliminating the need for hazardous experimental syntheses and analyses.

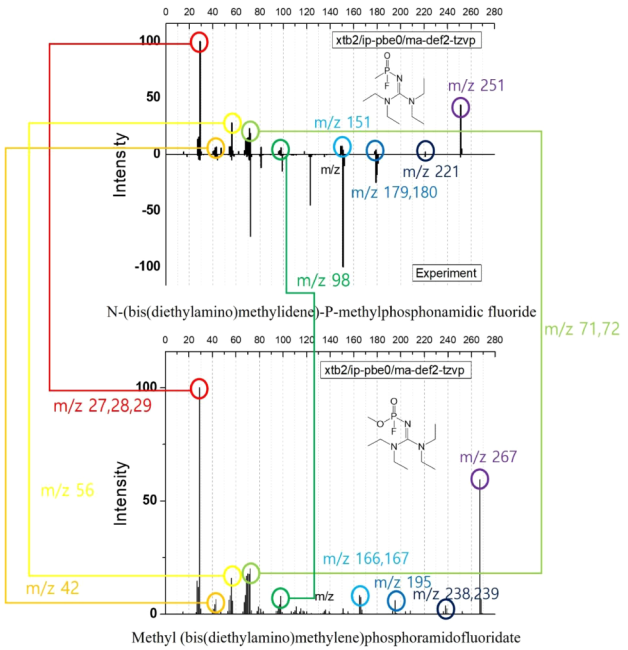
The results of QCxMS (x = EI) in Figure 5a, when compared with experimental values, show fragmentation starting from the ethyl group (m/z 27) near nitrogen, as extended in Figure 5b, up to a structure with an m/z value of 98.

As shown in Figure 5b, common fragmentations are observed around the nitrogen atom, with the ethyl group represented by m/z values ranging from 27 to 29, depending on the number of hydrogen atoms. The presence of four ethyl groups around the nitrogen atom appears to contribute to the observed intensity trend. The ethyl group including nitrogen is subsequently represented at m/z = 42. Following this, the fragmentation extends to include the ethyl group, nitrogen, and carbon, resulting in an m/z of 56. Two ethyl groups attached to nitrogen are observed at m/z values ranging from 71 to 72, corresponding to structures composed of two fragments adjacent to carbon. Finally, the m/z value of 98 represents a structure including $N(CH_3)_2$ along with carbon and nitrogen, originating from a fragmentation involving the double bond between carbon and nitrogen. This structure, which excludes two ethyl groups, is highlighted in green. Below m/z 100, as seen in Figure 5b, the spectra exhibit common structural fingerprints. However, interestingly, above m/z 100, the molecular structures exhibit distinct fingerprints, allowing for differentiation between the molecules. Figure 5c,d clearly highlights the differences between **compound 1** and **compound 5**. These differences arise from the previously mentioned substitution of a methyl group with a methoxy group, leading to a molecular weight difference equivalent to the atomic mass of oxygen.

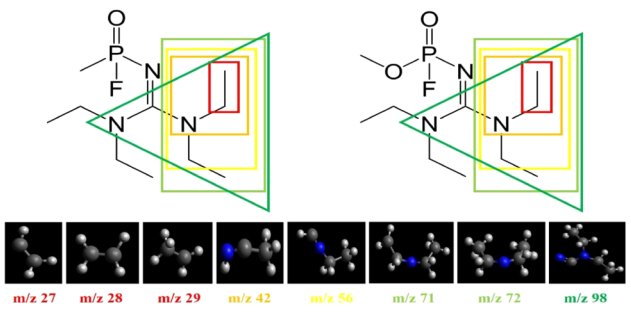
In Figure 5c, the m/z values range from 151 to 251 in the experimental and calculated results (experimental/calcd), while in Figure 5d (prediction), the m/z values are observed from 166 to 267. The structural features of the molecule are represented by m/z values that include phosphine-containing structures. For m/z 151, the structure features phosphine with a methyl group, while m/z 166 to 167 is characterized by the presence of a methoxy group. At m/z 180, an ethyl group is added to the structure compared to m/z 151, and the same applies to m/z 195, which is derived from m/z 166 to 167. Subsequently, at m/z 221 and 238−239, ethyl groups are removed, and finally, m/z 251 and 267 represent the molecule itself.

In conclusion, Figure 5 analyzes the fragmentation trends based on ma-def2-tzvp for both experimental/calculative and (prediction) cases. Detailed structures are presented in Figures S1 and S2, and the overall trend indicates that the m/z values below 100 for Novichok molecules are represented by structures involving two $N(CH_3)_2$ groups attached to a $N{=}C$ group. In contrast, for m/z values above 100, the differences in the electron ionization spectrum of the molecules can be distinguished by the presence of two $N(CH_3)_2$ groups and the

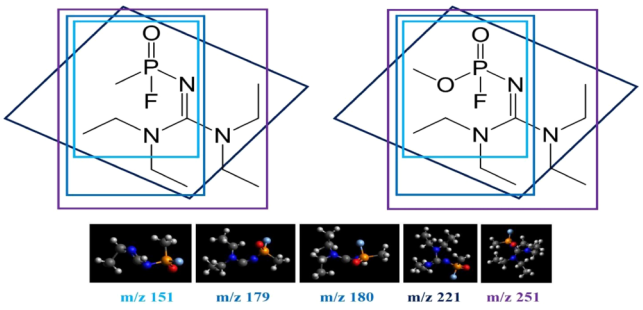
https://doi.org/10.1021/acsmeasuresciau.5c00026
ACS Meas. Sci. Au 2025, 5, 378−387



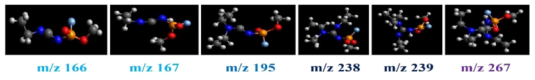
(a) Overlaid mass spectra of **Compound 1** and **Compound 5**, showing QCxMS spectrum ((+) intensity) and experimental spectrum((-)spectrum)



(b) The common Fragmentations of **Compound 1** and **Compound 5**



(c) Fragmentation of **Compound 1** (Exp./Cal. Analysis)



(d) Fragmentation of **Compound 5** (Prediction)

Figure 5. Peak and fragmentation analysis of **compound 1** and **compound 5** using QCxMS (x = EI) and experimental spectrum. Individual fragment peaks are color-coded as follows: red (m/z 27–29, ethyl group), orange (m/z 42, ethyl + nitrogen), yellow (m/z 56, ethyl + carbon + nitrogen), light green (m/z71–72, double ethyl adjacent to nitrogen), green (m/z 98, $N(CH_3)_2$ + C═N), sky blue (m/z 151/166–167), blue (m/z 180/195), navy (m/z 221/238–239), and purple (251/267).

presence of an O═P−F group, influenced by methyl and methoxy groups.

As shown in the analysis from Figure 5, fragments with common structures were identified in the mass spectrum for the molecules in Figure 1b–d. In Figure 6b, the three molecules exhibit a fragmentation pathway starting from the ethyl group near nitrogen (m/z 29) and extending to the cleavage of the bond between nitrogen and phosphorus (m/z 113). This reveals that fragments with m/z values below 120 exhibit common fragmentation patterns. In Figure 6b, a common feature is observed at m/z 29, corresponding to the ethyl group, showing a trend similar to that in Figure 5. Next, m/z 42 represents the structure extending to the nitrogen attached to the ethyl group. At m/z 57, the structure includes $N-CH_3$ along with carbon. Additionally, m/z 70–71, indicated in light green, corresponds to $N(CH_3)_2$. m/z 98 and m/z 113 are depicted as fragments resulting from the cleavage between phosphorus and nitrogen. The case where the methyl group is detached is highlighted in green, while the case where the methyl group remains intact is highlighted in light blue.

As illustrated in Figure 6c–e, the m/z values increase in correspondence with the molecular weights of the substituents: methyl, methoxy, and ethoxy groups. This characteristic fragmentation pattern is unique to each molecule, with m/z values above 120 distinctly reflecting their respective molecular weights. The conclusion from Figure 6, similar to Figure 5c,d, is that fragments with m/z values above 120 containing O═P−F exhibit characteristics unique to Novichok molecules. These fragments are expected to be helpful in analyzing the specific m/z peaks that reveal the distinct properties of the molecules.

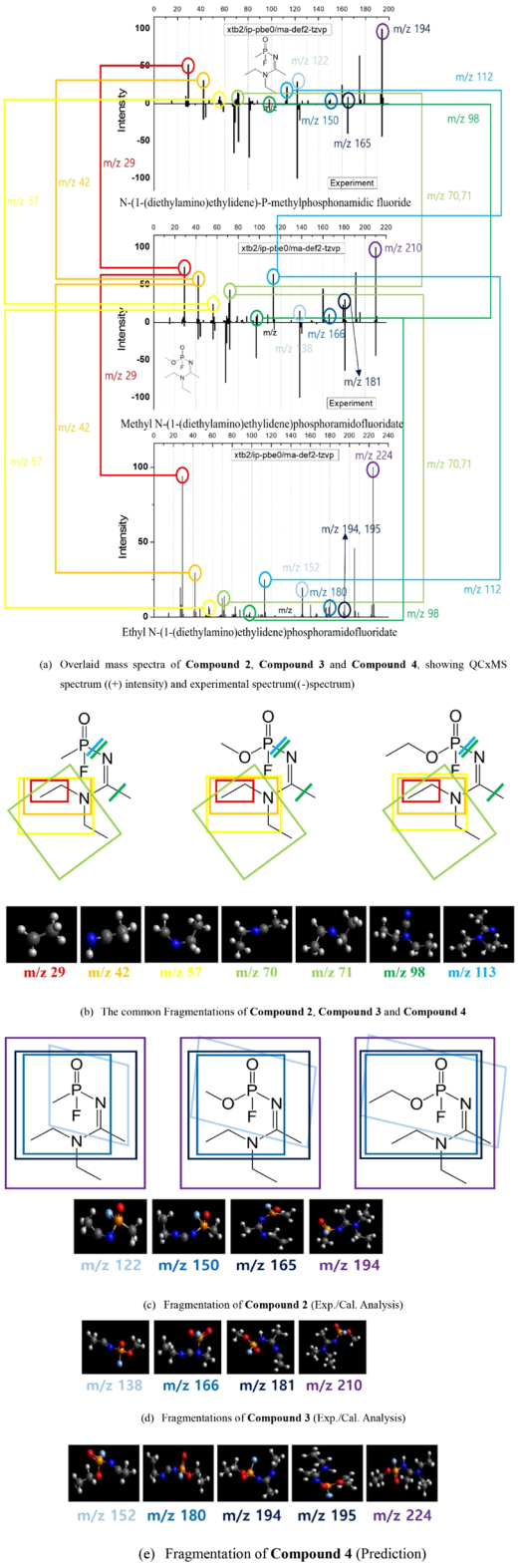
Figure S2 shows the analysis results of **compound 6** and **compound 7**, performed using the ma-def2-tzvp basis set, as in Figures 5 and 6. It presents all of the predicted fragmentations based on this analysis. Although the spectra in Figure 4c,d do not compare the relative peaks of the molecules, it is expected that the predicted mass spectra in Figure 4 will closely resemble the experimental spectra, consistent with the high matching scores obtained using the advanced basis set.

4. CONCLUSIONS

The rapid identification of chemical warfare agents, particularly novel Novichok variants, remains a critical challenge in global security and chemical defense. The traditional approach of building comprehensive spectral libraries through experimental synthesis and analysis is severely constrained by the extreme toxicity of these compounds, high costs, and limited availability of specialized facilities. This study addresses these challenges by advancing the computational prediction of mass spectra through QCxMS (x = EI).

Our research has yielded insights that significantly advance the field of computational mass spectral prediction for complex chemical warfare agents. Through a systematic investigation of basis set effects, we demonstrated that the advanced ma-def2-tzvp basis set consistently provides superior predictive performance compared to conventional basis sets while maintaining the same PBE0 functionals for IP calculations. Although the improvement in prediction accuracy is modest in absolute terms, it represents a meaningful advancement in our ability to computationally predict mass spectra for these complex molecules. The systematic analysis of fragmentation patterns has revealed important structure-spectrum relation-

https://doi.org/10.1021/acsmeasuresciau.5c00026
ACS Meas. Sci. Au 2025, 5, 378–387



(a) Overlaid mass spectra of **Compound 2**, **Compound 3** and **Compound 4**, showing QCxMS spectrum ((+) intensity) and experimental spectrum((-)spectrum)

(b) The common Fragmentations of **Compound 2**, **Compound 3** and **Compound 4**

(c) Fragmentation of **Compound 2** (Exp./Cal. Analysis)

(d) Fragmentations of **Compound 3** (Exp./Cal. Analysis)

(e) Fragmentation of **Compound 4** (Prediction)

Figure 6. Peak and fragmentation analysis of **compound 2**, **compound 3**, and **compound 4** using QCxMS (x = EI) and experimental spectrum. Individual fragment peaks are color-coded as follows: Red (*m*/*z* 29, ethyl group), orange (*m*/*z* 42, ethyl + nitrogen), yellow (*m*/*z* 57, ethyl + carbon + nitrogen), light green (m/z71−72, double ethyl adjacent to nitrogen), green (*m*/*z* 98, $N(CH_3)_2$ + C═N), sky blue (*m*/*z* 113, $N(CH_3)_2$-$C(CH_3)$═N), light sky blue (*m*/*z* 122/138/152), blue (*m*/*z* 150/166/180), navy (*m*/*z* 165/181/194−195), and purple (194/210/224).

ships in the Novichok compounds. Our work established clear correlations between specific structural features and their mass spectral signatures, particularly in the behavior of methyl, methoxy, and ethoxy groups bound to phosphine at higher *m*/*z* values and the distinctive patterns created by ethyl groups attached to nitrogen in guanidine and amidine structures at lower *m*/*z* values. This deeper understanding of fragmentation mechanisms has enabled us to predict the mass spectra of novel structural variants without requiring their physical synthesis. The matching scores achieved in this study, ranging from 0.158 to 0.191, while indicating room for improvement, should be considered within the broader context of the molecular complexity involved and the critical importance of developing any predictive capability for these dangerous compounds. These results, though not perfect, represent a significant step toward establishing reliable computational alternatives to experimental analysis.

Our findings suggest several promising avenues for future research in this field. The methodology could be enhanced through the exploration of additional advanced basis sets and functional combinations, potentially incorporating machine learning approaches to improve prediction accuracy. The development of more sophisticated fragmentation pattern analysis methods could further refine our predictive capabilities, and the methodology could be extended to encompass a broader range of chemical warfare agents and their degradation products. Perhaps most significantly, this work demonstrates the feasibility of using computational methods to predict the mass spectra of highly toxic compounds, potentially reducing the need for dangerous experimental work. As computational capabilities continue to advance, this approach may become an increasingly valuable tool in chemical defense, allowing the rapid identification of new threats without the risks associated with compound synthesis and analysis. While our study focused specifically on Novichok agents, the framework we have established provides a foundation for broader applications in predicting the mass spectra of other hazardous compounds where experimental analysis is impractical or dangerous.

■ ASSOCIATED CONTENT

Supporting Information

The Supporting Information is available free of charge at https://pubs.acs.org/doi/10.1021/acsmeasuresciau.5c00026.

Detailed comparison of experimental and calculated mass spectra for Novichok compounds, comprehensive visualization of molecular fragment structures corresponding to specific *m*/*z* values, graphical representation of mass spectral patterns with structural assignments, and complete fragmentation analysis of all seven compounds using the ma-def2-tzvp basis set (PDF)

■ AUTHOR INFORMATION

Corresponding Authors

Seungbum Jo − *Accident prevention and assessment Division, National Institute of Chemical Safety, Cheongju 28164, Republic of Korea*; Email: sebujo@korea.kr

Keunhong Jeong − *Department of Chemistry, Korea Military Academy, Seoul 01805, Republic of Korea*; orcid.org/0000-0003-1485-7235; Email: doas1 mind@kma.ac.kr

https://doi.org/10.1021/acsmeasuresciau.5c00026
ACS Meas. Sci. Au 2025, 5, 378−387

Authors

Sungsoo Kim − *School of Energy Systems Engineering, Chung-Ang University, Dongjak-Gu, Seoul 06974, Republic of Korea*

Moon Sik Shin − *ROK Chemical, Biological and Radiological Defense Research Institute, Seocho-gu, Seoul 06790, Republic of Korea*

Seonghoon Hong − *ROK Chemical, Biological and Radiological Defense Research Institute, Seocho-gu, Seoul 06790, Republic of Korea*

Janghyuk Moon − *School of Energy Systems Engineering, Chung-Ang University, Dongjak-Gu, Seoul 06974, Republic of Korea;* orcid.org/0000-0002-8965-1971

Complete contact information is available at: https://pubs.acs.org/10.1021/acsmeasuresciau.5c00026

Author Contributions

CRediT: **Sungsoo Kim** data curation, formal analysis, investigation, methodology, validation, writing - original draft, writing - review & editing; **Seonghoon Hong** formal analysis, investigation, writing - original draft.

Notes

The authors declare no competing financial interest.

■ ACKNOWLEDGMENTS

This research was funded by a National Research Foundation of Korea (NRF) grant, funded by the Korean government (Ministry of Science and ICT), RS-2024-00422023 and RS-2025-00519428.

■ REFERENCES

(1) Jeong, K.; Choi, J. Theoretical Study on the Toxicity of 'Novichok' Agent Candidates. *R. Soc. Open Sci.* **2019**, *6* (8), 190414.

(2) Chai, P. R.; Hayes, B. D.; Erickson, T. B.; Boyer, E. W. Novichok Agents: A Historical, Current, and Toxicological Perspective. *Toxicol. Commun.* **2018**, *2* (1), 45−48.

(3) Nepovimova, E.; Kuca, K. Chemical Warfare Agent NOVICHOK - Mini-Review of Available Data. *Food Chem. Toxicol.* **2018**, *121*, 343−350.

(4) Goldsmith, M.; Ashani, Y. Catalytic Bioscavengers as Countermeasures against Organophosphate Nerve Agents. *Chem.-Biol. Interact.* **2018**, *292*, 50−64.

(5) Santos, M. C.; Botelho, F. D.; Gonçalves, A. S.; Kuca, K.; Nepovimova, E.; Cavalcante, S. F. A.; Lima, A. L. S.; França, T. C. C. Theoretical Assessment of the Performances of Commercial Oximes on the Reactivation of Acetylcholinesterase Inhibited by the Nerve Agent A-242 (Novichok). *Food Chem. Toxicol.* **2022**, *165*, 113084.

(6) Pope, C. N. ORGANOPHOSPHORUS PESTICIDES: DO THEY ALL HAVE THE SAME MECHANISM OF TOXICITY? *J. Toxicol. Environ. Health B* **1999**, *2* (2), 161−181.

(7) Chandar, N. B.; Lo, R.; Ganguly, B. Quantum Chemical and Steered Molecular Dynamics Studies for One Pot Solution to Reactivate Aged Acetylcholinesterase with Alkylator Oxime. *Chem. Biol. Interact.* **2014**, *223*, 58−68.

(8) Lo, R.; Ganguly, B. Can Hydroxylamine Be a More Potent Nucleophile for the Reactivation of Tabun-Inhibited AChE than Prototype Oxime Drugs? An Answer Derived from Quantum Chemical and Steered Molecular Dynamics Studies. *Mol. BioSyst.* **2014**, *10* (9), 2368−2383.

(9) D'Agostino, P. A. Chapter 25 Chemical Warfare Agents. In *Handbook of Analytical Separations*, Bogusz, M. J., Ed.; Elsevier, 2008; Vol. *6*, pp. 839−872. DOI: .

(10) Hooijschuur, E. W. J.; Hulst, A. G.; de Jong, A. L.; de Reuver, L. P.; van Krimpen, S. H.; van Baar, B. L. M.; Wils, E. R. J.; Kientz, C. E.; ATh Brinkman, U. Identification of chemicals related to the chemical weapons convention during an interlaboratory proficiency test. *TrAC, Trends Anal. Chem.* **2002**, *21* (2), 116−130.

(11) Wang, S.; Lin, C.; Zhao, L.; Gong, X.; Zhang, M.; Zhang, H.; Hu, P. Identifying Isomers in Chinese Traditional Medicine via Density Functional Theory and Ion Fragmentation Simulation Software QCxMS. *J. Chromatogr. A* **2024**, *1730*, 465122.

(12) Carvalho-Silva, T.; Modesto-Costa, L.; Borges, C. V. N.; Cavalcante, S. F. A.; Sousa, R. B.; Lima, A. L. S.; Borges, I. Synthesis, Experimental and Molecular Dynamics Simulation of the ESI-CID Spectrum of the Nerve Agent Novichok Analog O-2-Methoxyethyl N-[Bis(Dimethylamino)Methylidene]-P-Methylphosphonamidate. *Int. J. Mass Spectrom.* **2023**, *490*, 117087.

(13) OPCW. *Guidelines for Schedules of Chemicals*. 2022, https://apps.opcw.org/cas/default.aspx. accessed 9 May 2025.

(14) OPCW. *Convention on the Prohibition of the Development, Production, Stockpiling and Use of Chemical Weapons and on Their Destruction*. 2020, https://www.opcw.org/sites/default/files/documents/CWC/CWC_en.pdf. accessed 9 May 2025.

(15) OPCW. *Consolidated Text of Adopted Changes to Schedule 1 of the Annex on Chemicals to the Chemical Weapons Convention*. 2025, https://www.opcw.org/chemical-weapons-convention/annexes/annex-chemicals/schedule-1. accessed 9 May 2025.

(16) Chernicharo, F. C. S.; Modesto-Costa, L.; Borges, I. Simulation of the electron ionization mass spectra of the Novichok nerve agent. *J. Mass Spectrom.* **2021**, *56* (5), No. e4779.

(17) Valdez, C. A.; Leif, R. N.; Hok, S.; Hart, B. R. Analysis of Chemical Warfare Agents by Gas Chromatography−Mass Spectrometry: Methods for Their Direct Detection and Derivatization Approaches for the Analysis of Their Degradation Products. *Rev. Anal. Chem.* **2018**, *37* (1), 1−26.

(18) Alcaraz, A.Gas Chromatography/Mass Spectrometry in Analysis of Chemicals Relevant to the Chemical Weapons Convention*Encyclopedia Of Analytical Chemistry*John Wiley & Sons2012

(19) Podborsky, V.; Zavadilík, P.; Šafářová, L. Fragmentation of Tabun's Derivatives in Standard EI-MS Spectra. *Chem. Listy* **2019**, *113*, 168−178.

(20) Bauer, C. A.; Grimme, S. How to Compute Electron Ionization Mass Spectra from First Principles. *J. Phys. Chem. A* **2016**, *120* (21), 3755−3766.

(21) Ásgeirsson, V.; Bauer, C. A.; Grimme, S. Quantum Chemical Calculation of Electron Ionization Mass Spectra for General Organic and Inorganic Molecules. *Chem. Sci.* **2017**, *8* (7), 4879−4895.

(22) Chernicharo, F. C. S.; Modesto-Costa, L.; Borges, I. Simulation of the Electron Ionization Mass Spectra of the Novichok Nerve Agent. *J. Mass Spectrom.* **2021**, *56* (9), No. e4779.

(23) Koopman, J.; Grimme, S. From QCEIMS to QCxMS: A Tool to Routinely Calculate CID Mass Spectra Using Molecular Dynamics. *J. Am. Soc. Mass Spectrom.* **2021**, *32* (7), 1735−1751.

(24) Becke, A. D. DENSITY-FUNCTIONAL THERMOCHEMISTRY.3. THE ROLE OF EXACT EXCHANGE. *J. Chem. Phys.* **1993**, *98* (7), 5648−5652.

(25) Wiberg, K. B. Basis Set Effects on Calculated Geometries: 6−311++G** vs. Aug-Cc-PVDZ. *J. Comput. Chem.* **2004**, *25* (11), 1342−1346.

(26) Chernicharo, F. C. S.; Modesto-Costa, L.; Borges, I. Molecular Dynamics Simulation of the Electron Ionization Mass Spectrum of Tabun. *J. Mass Spectrom.* **2020**, *55* (6), No. e4513.

(27) Bannwarth, C.; Ehlert, S.; Grimme, S. GFN2-XTB - An Accurate and Broadly Parametrized Self-Consistent Tight-Binding Quantum Chemical Method with Multipole Electrostatics and Density-Dependent Dispersion Contributions. *J. Chem. Theory Comput.* **2019**, *15* (3), 1652−1671.

(28) Ernzerhof, M.; Scuseria, G. E. Assessment of the Perdew−Burke−Ernzerhof Exchange-Correlation Functional. *J. Chem. Phys.* **1999**, *110* (11), 5029−5036.

(29) Grimme, S.; Antony, J.; Ehrlich, S.; Krieg, H. A Consistent and Accurate Ab Initio Parametrization of Density Functional Dispersion

Correction (DFT-D) for the 94 Elements H-Pu. *J. Chem. Phys.* **2010**, *132* (15), 154104.
(30) Weigend, F.; Ahlrichs, R. Balanced Basis Sets of Split Valence, Triple Zeta Valence and Quadruple Valence Quality for H to Rn: Design and Assessment of Accuracy. *Phys. Chem. Chem. Phys.* **2005**, *7* (18), 3297−3305.
(31) Neese, F.; Wennmohs, F.; Becker, U.; Riplinger, C. The ORCA Quantum Chemistry Program Package. *J. Chem. Phys.* **2020**, *152* (22), 224108.
(32) Zheng, J.; Xu, X.; Truhlar, D. G. Minimally Augmented Karlsruhe Basis Sets. *Theor. Chem. Acc.* **2011**, *128* (3), 295−305.

https://doi.org/10.1021/acsmeasuresciau.5c00026
ACS Meas. Sci. Au 2025, 5, 378−387